

Temporal Action Localization for Inertial-based Human Activity Recognition

MARIUS BOCK, University of Siegen, Germany

MICHAEL MOELLER, University of Siegen, Germany

KRISTOF VAN LAERHOVEN, University of Siegen, Germany

A persistent trend in Deep Learning has been the applicability of machine learning concepts to other areas than originally introduced for. As of today, state-of-the-art activity recognition from wearable sensors relies on classifiers being trained on fixed windows of data. Contrarily, video-based Human Activity Recognition has followed a segment-based prediction approach, localizing activity occurrences from start to end. This paper is the first to systematically demonstrate the applicability of state-of-the-art TAL models for wearable Human Activity Recognition (HAR) using raw inertial data as input. Our results show that state-of-the-art TAL models are able to outperform popular inertial models on 4 out of 6 wearable activity recognition benchmark datasets, with improvements ranging as much as 25% in F1-score. Introducing the TAL community's most popular metric to inertial-based HAR, namely mean Average Precision, our analysis shows that TAL models are able to produce more coherent segments along with an overall higher NULL-class accuracy across all datasets. Being the first to provide such an analysis, the TAL community offers an interesting new perspective to inertial-based HAR with yet to be explored design choices and training concepts, which could be of significant value for the inertial-based HAR community.

CCS Concepts: • **Human-centered computing** → **Ubiquitous and mobile computing design and evaluation methods**; • **Computing methodologies** → **Neural networks**.

Additional Key Words and Phrases: Deep Learning, Inertial-based Human Activity Recognition, Body-worn Sensors, Temporal Action Localization

1 INTRODUCTION

The recognition of performed activities through wearable sensors such as IMUs has shown to be of significant value in areas such as health care or the support of complex work processes [7]. Deep Learning has established itself as the de facto standard in wearable, inertial-based Human Activity Recognition (HAR), consistently outperforming classical Machine Learning approaches in recognition performance. A persistent trend in Deep Learning has been the applicability of machine learning concepts such as self-attention [51] to other areas and application scenarios than originally introduced for. With significant progress having been made since the introduction of deep neural architectures such as the DeepConvLSTM [35], researchers have followed this trend and continuously worked on improving the architectural design of networks by incorporating newly introduced techniques (see e.g., [67]).

A promising recent approach in video-based Human Activity Recognition (HAR) is Temporal Action Localization (TAL), which aims to locate activity segments, defined by a class label, start, and end point, within an untrimmed video. Even though introduced architectures have almost doubled in performance over the last 5 years on existing datasets like THUMOS-14 [21], results on large corpora such as EPIC-KITCHENS-100 [14] and Ego4D [17] show that the prediction problem is far from being saturated. Recently, Zhang et al. [62] introduced the ActionFormer, an end-to-end, single-stage TAL model utilizing transformer-based layers. Being the first of its kind, the ActionFormer along with extensions of it [43, 48] are as of today holding top ranks in

Authors' addresses: [Marius Bock](mailto:marius.bock@uni-siegen.de), marius.bock@uni-siegen.de, University of Siegen, Hölderlinstrasse 3, Siegen, North Rhine-Westphalia, Germany, 57076; [Michael Moeller](mailto:michael.moeller@uni-siegen.de), michael.moeller@uni-siegen.de, University of Siegen, Hölderlinstrasse 3, Siegen, North Rhine-Westphalia, Germany, 57076; [Kristof Van Laerhoven](mailto:kvl@eti.uni-siegen.de), kvl@eti.uni-siegen.de, University of Siegen, Hölderlinstrasse 3, Siegen, North Rhine-Westphalia, Germany, 57076.

prediction performance on a multitude of TAL benchmark datasets. Despite sharing a mutual goal, the TAL community evaluates their approaches differently from the inertial community, using mean Average Precision (mAP) as opposed to traditional classification metrics like F1-score or accuracy. TAL models have recently been shown to be capable of being trained using raw inertial data [5], marking the first instance of such vision-based models being applied in the context of inertial-based HAR. When compared with popular inertial models, results on one particular dataset have already shown that TAL models can produce more coherent and less fragmented predictions while maintaining performance in terms of traditional classification metrics.

Setting out to further examine the applicability of Temporal Action Localization for inertial-based HAR, our contributions in this paper are three-fold:

- (1) We demonstrate the capabilities of a novel approach to inertial-based HAR, being single-stage TAL, to outperform popular inertial models on four out of six wearable activity recognition benchmark datasets.
- (2) Complementing traditional, frame-wise classification metrics, we introduce a set of unexplored, segment-based evaluation metrics for inertial-based HAR, which are based around the scalar evaluation metric mean Average Precision [2].
- (3) We name differences and similarities between models originating from both communities, highlighting applied concepts that TAL models use to produce coherent segments along with a high NULL-class accuracy.

2 RELATED WORK

Inertial-based Human Activity Recognition. With on-body sensors providing a robust and non-intrusive way to monitor participants along long stretches of time, research conducted in the area of inertial-based HAR has worked towards the automatic interpretation of one or multiple sensor streams to reliably detect activities e.g. in the context of providing medical support or providing guidance during complex work processes [7]. With deep neural networks having established themselves as the de facto standard in inertial-based HAR, the DeepConvLSTM [35] as well as models introduced at a later point all follow a similar prediction scenario design applying a sliding window approach which groups concurrent data points for classification. In their original publication Ordóñez and Roggen [35] have found a combination of convolutional and recurrent layers to produce competitive results, with the idea being to model temporal dependencies amongst automatically extracted discriminative features within a sliding window in order to classify it correctly as one of the N activity classes or, if applicable, NULL-class. Building up on the idea of combining these two types of layers, researchers have worked on extending the original DeepConvLSTM or have introduced their own architectural designs [1, 4, 11–13, 28, 32, 33, 37, 50, 55–58, 64, 67]. A simple modification of the DeepConvLSTM is the shallow DeepConvLSTM [4]. Contradicting the popular belief that one needs at least two recurrent layers when dealing with time series data [22], Bock et al. [4] demonstrated that removing the second LSTM layer within the original DeepConvLSTM architecture, results in significant increases in predictive performance on a multitude of HAR benchmark datasets while also decreasing the number of learnable parameters. Furthermore, with the original DeepConvLSTM only being able to learn temporal dependencies within a sliding window, the shallow DeepConvLSTM applies the LSTM across batches, effectively making the batches the sequence which is to be learned by the LSTM. This dimension-flip, along with a non-shuffled training dataset, enables the architecture to learn temporal dependencies amongst a batched input. The same year as the shallow DeepConvLSTM, Abedin et al. [1] introduced Attend-and-Discriminate, a deep neural network architecture following the idea of the original

DeepConvLSTM by combining both convolutional and recurrent layers, yet further adding a cross-channel interaction encoder using self-attention as well as attention mechanism to the recurrent parts of the network. In 2022 Zhou et al. [67] proposed TinyHAR, a lightweight HAR model that uses a transformer encoder block along with means of cross-channel fusion via a fully connected layer and a final self-attention layer which aims to learn the contribution of each outputted time step produced by the recurrent parts individually.

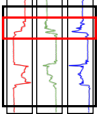
Video-based Human Activity Recognition. Classifying videos in the context of Human Activity Recognition can broadly be categorized into three main application scenarios: Action Recognition, which aims to classify trimmed videos into one of C activity classes; Action Anticipation, which aims to predict the next likely activities after observing a preceding video sequence; and Temporal Action Localization (TAL), which seeks to identify and locate all activity segments within an untrimmed video. With the inertial-based benchmark datasets consisting of a multitude of activities, TAL is to be considered most comparable to inertial-based HAR. Unlike popular inertial architectures though, TAL models aim to predict all segments within an untrimmed video at once. Existing TAL methods can broadly be categorized into two categories: two-stage and one-stage recognition systems. Two-stage recognition system [3, 16, 24, 26, 29, 38, 45, 47, 59, 61, 65, 66, 68] divide the process of identifying actions within an untrimmed video into two subtasks. First, during proposal generation, candidate segments are generated, which are then, during the second step, classified into one of C activity classes and iteratively refined regarding their start and end times. Contrarily, single-stage models [10, 25, 27, 30, 31, 34, 43, 44, 48, 60, 62] do not rely on activity proposals, directly aiming to localize segments along their class label and refined boundaries. In 2022 Zhang et al. [62] introduced the ActionFormer, a lightweight, single-stage TAL model which unlike previously introduced single-stage architectures does not rely on pre-defined anchor windows. In line with the success of transformers in other research fields, Zhang et al. [62] demonstrated their applicability for TAL, outperforming previously held benchmarks on several TAL datasets [14, 19, 21] by a significant margin. Surprisingly, a year later the TemporalMaxer suggested removing transformer layers within the ActionFormer arguing feature embeddings are already discriminative enough [48]. Though being more lightweight than the ActionFormer, the TemporalMaxer showed to outperform its precedent during benchmark analysis. Similar to the TemporalMaxer, Shi et al. [43] introduced TriDet, which suggested altering the ActionFormer in two ways. First, to mitigate the risk of rank-loss, self-attention layers are replaced with SGP layers. Second, the regression head in the decoder is replaced with a Trident head, which improves imprecise boundary predictions via an estimated relative probability distribution around each timestamp’s activity boundaries.

3 TEMPORAL ACTION LOCALIZATION FOR INERTIAL-BASED HAR

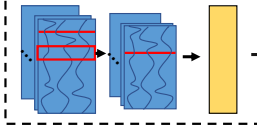
As the inertial-based HAR and TAL communities deal with inherently different modalities, both communities have developed distinct predictive pipelines and algorithms tailored to the challenges and characteristics of their respective modalities (see Figure 1). In the following section, we will provide detailed descriptions of the two different predictive pipelines and demonstrate how vision-based TAL models can be applied to a previously unexplored modality – inertial data. Furthermore, we provide a detailed overview of the architectural design of three popular single-stage TAL models [43, 48, 62] highlighting similarities as well as differences of the architectures compared to models originating from the inertial-based HAR community.

3.1 Inertial-based HAR vs. Temporal Action Localization

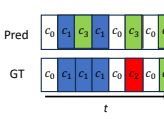
Problem definition. The objective of both inertial activity recognition and TAL is to predict all activities present in an untrimmed timeline. Given an input data stream X of a sample participant,

Inertial Activity Recognition:**Sliding Inertial-Windows**e.g. $[N \times 1 \text{ sec.} \times \# \text{Axes}]$ **DL Model**

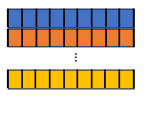
E.g. DeepConvLSTM

**Per-window classification**

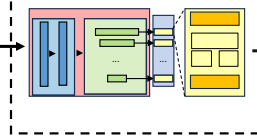
[N activity labels]

Accuracy,
F1-score,
etc.**(Single-stage) Temporal Action Localization:****Sliding Video-Windows**e.g. $[N \times 1 \text{ sec.}]$

Feature extraction

**Feature Embeddings**e.g. $[N \times 2048]$ **DL Model**

E.g. ActionFormer

**Segment prediction**

[M (activity, start, end)-triplets]

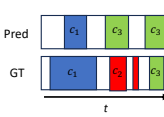
mAP @
different tIoU
thresholds

Fig. 1. Overview of the prediction pipelines applied in inertial-based activity recognition and single-stage Temporal Action Localization (TAL). Both apply a sliding window to divide input data into windows of a certain duration (e.g. one second). TAL models do not use raw data as input but are applied on per-clip, pre-extracted feature embeddings. Inertial activity recognition models predict activity labels for each sliding window, which are used for calculating classification metrics such as accuracy and F1. TAL models predict activity segments, defined by a label, start and end points, and are evaluated with mean Average Precision (mAP) applied at different temporal Intersection over Union (tIoU) thresholds.

both the inertial and TAL communities start by applying a sliding window approach which shifts over X , dividing the input data into windows, e.g. of one second duration with a 50% overlap between consecutive windows. This process results in $X = \{x_1, x_2, \dots, x_T\}$ being discretized into $t = \{0, 1, \dots, T\}$ time steps, where T is the number of windows for each participant. It is important to note that the TAL models do not use raw data as input, but are instead trained using feature embeddings extracted from each individual sliding video clip, which are extracted using pretrained methods such as [8]. That is, in the case of TAL, x_t represents a one-dimensional feature embedding vector associated with the video clip at time step t . In case of inertial-based activity recognition, x_t represents a two-dimensional matrix of size $\mathbb{R}^{W \times S}$, where W is the number of samples within a window, and S is the number of sensor axes present in the sensor data.

Given all sliding windows associated with an untrimmed sequence, inertial activity recognition models aim to predict an activity label a_t for each sliding window x_t , where a belongs to a predefined set of activity labels, $a_t \in 1, \dots, C$. To do so, the sliding windows are batched and fed through e.g. a deep neural network, such as the DeepConvLSTM [35]. The resulting activity labels for each window are then compared to the true activity labels from the ground truth data, and classification metrics like accuracy or F1-score are calculated. Contrarily, TAL models aim to identify and localize segments of actions within the untrimmed data stream, which can span across multiple windows. To achieve this algorithms are trained to predict activity segments $Y = \{y_1, y_2, \dots, y_N\}$ using a collection of feature embeddings X as input, where N varies across participants. Each activity instance $y_i = (s_i, e_i, a_i)$ is defined by its starting time s_i (onset), ending time e_i (offset) and its associated activity label a_i , where $s_i \in [0, T]$, $e_i \in [0, T]$ and $a_i \in \{1, \dots, C\}$.

Evaluation metrics. As predictive outcomes of inertial activity recognition and TAL differ, both communities have adopted different evaluation metrics. In case of the inertial community, the

problem of recognizing activities is translated to a per-window classification problem, where each window represents an instance to be classified into one of C classes. Therefore, most researchers assess their algorithms based on traditional classification measures, including recall (R), precision (P), and F1-score ($F1$). In order to calculate these activity-wise metrics one first needs to calculate activity-wise *True Positives* (TP), *False Positives* (FP), *True Negatives* (TN) and *False Negatives* (FN). For a given activity class $i \in \{1, \dots, C\}$, a predicted activity label is to be treated as:

- TP of class i (TP_i): the predicted and ground truth label are equal to i
- FP of class i (FP_i): the predicted label is equal to i , yet the ground truth is not
- TN of class i (TN_i): the predicted and ground truth label are not equal to i
- FN of class i (FN_i): the predicted label is not equal to i , yet the ground truth is

Calculating TP , FP , TN and FN counts of all activities then allows to calculate the per-class classification metrics, which are defined as:

$$P_i = \frac{TP_i}{TP_i + FP_i} \quad (1) \quad R_i = \frac{TP_i}{TP_i + FN_i} \quad (2) \quad F1_i = \frac{2 \cdot P_i \times R_i}{P_i + R_i} \quad (3)$$

To account for the continuous nature of activity recognition prediction streams, Ward et al. [52] introduced additional performance metrics to explicitly measure misalignment within predictions made by inertial-based activity recognition systems. According to the authors, calculating classification metrics such as precision and recall based on window-wise errors does not provide intuitive insights about the overall fragmentation and merging behavior of the prediction stream. The authors propose to further divide the class-wise counts of FP s and FN s into additional sub-categories based on their relative position within a segmented predictive stream. These misalignment sub-categories are:

- (1) *Underfill* (U_i): False Negatives of class i that occur at the start or end of an activity segment, effectively making the predicted segment shorter by starting later or finishing earlier than the corresponding ground truth segment of i .
- (2) *Deletion* (D_i): False Negatives of class i that correspond to a deleted event, i.e. a ground segment which is missed completely within the prediction stream.
- (3) *Fragmenting* (F_i): False Negatives of class i that occur in-between True Positive instances of class i , falsely splitting a coherent segment into two segments.
- (4) *Insertion* (I_i): False Positives of class i that correspond to a non-existent ground truth segment.
- (5) *Overfill* (O_i): False Positives of class i that occur at the start or end of an activity segment, effectively making the predicted segment longer by predicting an earlier start or later finish than the corresponding ground truth segment.
- (6) *Merge* (M_i): False Positives of class i that occur between two ground truth segments incorrectly merging the two segments into one coherent segment.

Calculating these six misalignment U , D , F , I , O and M counts of all activities then allows calculating the per-class misalignment ratios, which are defined as:

$$UR_i = \frac{U_i}{TN_i + FN_i} \quad (4) \quad DR_i = \frac{D_i}{TN_i + FN_i} \quad (5) \quad FR_i = \frac{F_i}{TN_i + FN_i} \quad (6)$$

$$IR_i = \frac{I_i}{TP_i + FP_i} \quad (7) \quad OR_i = \frac{O_i}{TP_i + FP_i} \quad (8) \quad MR_i = \frac{M_i}{TP_i + FP_i} \quad (9)$$

Inspired by measures applied during object detection, the TAL community assess algorithms based mean Average Precision (mAP) performance applied at different temporal Intersection over

Union (tIoU) thresholds. With a TAL model being trained to predict a set of activity segments Y , each predicted segment is compared with the ground truth activity segments within the complete input data stream of a participant. That is, given a predicted activity segment $y_p = (s_p, e_p, a_p)$ and a ground truth activity segment $y_g = (s_g, e_g, a_g)$, the two segments are considered to be either TP , FP , TN or FN based on the condition that the temporal intersection over union (tIoU) (overlap of the two segments divided by the union of the two segments) is greater than a predefined threshold, e.g., 0.5. Mean Average Precision is then calculated as:

$$mAP = \frac{1}{N} \sum_{a=1}^C AP_a, \quad (10)$$

where AP_i represents the area under the curve of the *Precision-Recall-Curve*, which is obtained by plotting a model's precision and recall values as a function of the model's confidence score threshold for a given class $a \in \{1, \dots, C\}$. More specifically, the mAP score at a tIoU threshold of, for example, 0.2 (mAP@0.2), is calculated as the mAP score assuming a required tIoU of 0.2 when calculating TP , FP , TN and TN counts. Typically, to assess the predictive performance of TAL models, mAP is calculated using a range of tIoU thresholds, which are then averaged. In case of this benchmark analysis we calculate mAP as mAP@(0.3:0.1:0.7), which equates to calculating the mAP@0.3, mAP@0.4, mAP@0.5, mAP@0.6 and mAP@0.7 and averaging the individual scores.

3.2 Vectorization of Inertial Data for TAL

As previously mentioned, the input data X used to train TAL models is a collection of feature embeddings. These embeddings are, for instance, extracted using some pre-trained method applied on each video clip. The resulting embeddings are 1-dimensional feature vectors that summarize information such as RGB and optical flow of the video clip (see, for example, Carreira and Zisserman [8]). Since both communities employ a sliding window approach but feed data to their models using different dimensions, Bock et al. [5] proposed a simple, yet effective preprocessing step. This step converts the 2-dimensional, windowed inertial data, as used by inertial architectures, into a 1-dimensional feature embedding suitable for training TAL models. The preprocessing method as detailed in Figure 2 involves concatenating the different sensor axes of each window, converting the input data to be a collection of 1-dimensional feature embedding vectors $\mathbf{x}_t \in \mathbb{R}^{1 \times WS}$ where W is the number of samples within a window, and S is the number of sensor axes. More specifically, given a sliding window $\mathbf{x}_{SW} \in \mathbb{R}^{W \times S}$, we vectorize the two-dimensional matrix as follows:

$$\mathbf{x}_{SW} = \begin{bmatrix} x_{11} & \dots & x_{1S} \\ \vdots & \ddots & \\ x_{W1} & & x_{WS} \end{bmatrix} \rightarrow \text{vec}(\mathbf{x}_{SW}) = \begin{bmatrix} x_{11} \\ \vdots \\ x_{1S} \\ x_{2S} \\ \vdots \\ x_{WS} \end{bmatrix} \quad (11)$$

3.3 Architectures Overview

In order to predict activity segments $Y = \{y_1, y_2, \dots, y_N\}$ within an input video, the ActionFormer, TemporalMaxer and TriDet model all follow the same sequence labeling problem formulation for action localization. That is, given a set of feature input vectors $X = \{\mathbf{x}_1, \mathbf{x}_2, \dots, \mathbf{x}_T\}$, a model aims to classify each timestamp's as either one of the activity categories C or as background (NULL-class)

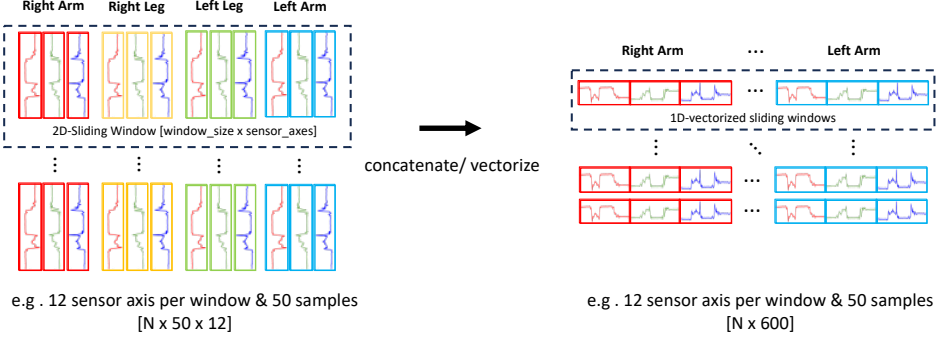


Fig. 2. Visualization of the applied vectorization on top of windowed inertial data assuming four 3D-inertial sensors and a sliding window size of 50 samples. Each 2D-sliding-window of size $[50 \times 12]$ is vectorized by concatenating each of the axes one after another. Resulting 1D-embedding vectors, being of size $[1 \times 600]$, can be used to train TAL models.

and regress the distance towards the timestamp’s corresponding segment’s start and end point. More specifically, given the input vectors X a model aims to learn to label the sequence as

$$X = \{\mathbf{x}_1, \mathbf{x}_2, \dots, \mathbf{x}_T\} \rightarrow \hat{Y} = \{\hat{y}_1, \hat{y}_2, \dots, \hat{y}_T\} \quad (12)$$

, where $\hat{y}_t = (p(a_t), d_t^s, d_t^e)$ at timestamp t is defined by a probability vector $p(a_t)$ indicating the class-wise probability of the timestamp being classified as one of the activity categories C and $d_t^s > 0$ and $d_t^e > 0$ being the distance between the current timestamp t and the current segment’s onset and offset. Note that d_t^s and d_t^e are not defined if the timestamp is to be classified as background. The sequence labeling formulation can then be easily decoded to activity segments as:

$$a_t = \arg \max p(a_t), \quad s_t = t - d_t^s, \quad \text{and} \quad e_t = t + d_t^e \quad (13)$$

ActionFormer. Introduced in 2022, the ActionFormer was among the first single-stage, anchor-free TAL models which followed a transformer-based design [62]. The architecture, depicted in Figure 3, follows an encoder-decoder structure that decomposes the previously defined task of learning to predict activity segments using a function f as $h \circ g$, where $g : X \rightarrow Z$ serves as the encoder and $h : Z \rightarrow \hat{Y}$ is the decoder. As the encoder Zhang et al. [62] employ a combination of convolutional layers and a transformer network. The convolutional layers, paired with ReLU activation functions, project each input feature vector \mathbf{x}_t into a D -dimensional space. To limit complexity, each layer of the transformer network applies alternating layers of multi-head local self-attention and MLP. To capture information at different temporal scales, the transformer network is structured in such a way that across its L layers, the initially embedded feature vector \mathbf{z}_0 at timestamp t is downsampled using a strided depthwise 1D-convolution.

After encoding the input sequence into a feature pyramid $Z = \{\mathbf{z}_1, \mathbf{z}_2, \dots, \mathbf{z}_L\}$, which captures information at various temporal scales, the decoder decodes the feature pyramid Z into sequence labels \hat{Y} . To do so, the decoder includes both a classification and regression head. The classification head, being 1D convolutional network complemented with layer normalization and ReLU activation, predicts for all L pyramid levels the probability vector $p(a_t)$ at each timestep t . The regression head, following the same design, predicts the onset (d_t^s) and offset distance (d_t^e) at all pyramid levels L for each timestamp t . Note that for both the classification and regression heads, parameters are shared across pyramid levels and output regression ranges are pre-specified per pyramid level. Finally, to

reduce overlapping instances and create a final set of predicted activity segments, the obtained predictions across all pyramid levels are postprocessed using Soft-NMS [6].

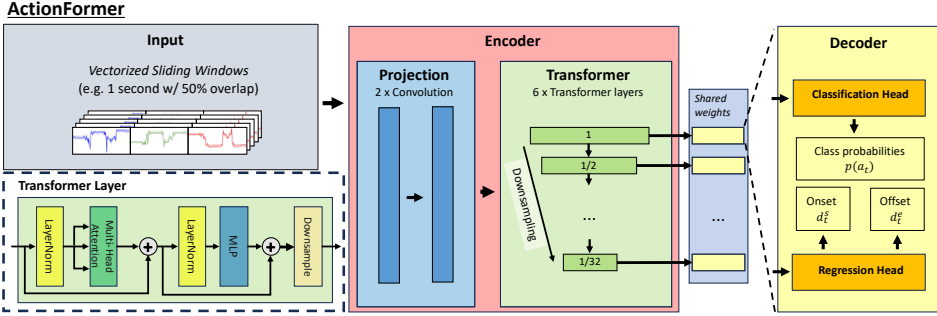


Fig. 3. Architecture overview of the ActionFormer proposed by Zhang et al. [62]. The architecture follows an encoder-decoder structure. The encoder, comprising of a projection using convolutional layers and a transformer network, encodes input sequences into a feature pyramid, which captures information at various temporal scales. The decoder, consisting of a classification and regression head, then decodes each timestamp within the feature pyramid to sequence labels, i.e. a class probability vector and the timestamp’s activity onset and offset distance. Note that weights of the decoder are shared across pyramid levels.

TemporalMaxer. Building upon the architectural design of the Actionformer [62], the TemporalMaxer proposed by Tang et al. [48] suggests modifying the encoder of the ActionFormer to employ solely max pooling and remove any multi-head attention layers (see Figure 4). According to the authors, the removal of the transformer-based layers does not come at the cost of a lost in information, as the extracted feature embeddings X outputted by the projection layer are already discriminative enough to achieve state-of-the-art predictive performance. Same as the ActionFormer, the weights of both the classification and regression heads within the TemporalMaxer are shared across pyramid levels, output regression ranges are pre-specified per pyramid level, and to create a final set of predicted activity segments, obtained predictions across all pyramid levels are postprocessed using Soft-NMS [6].

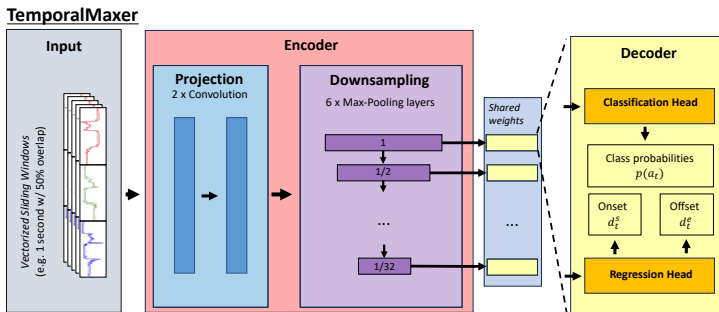


Fig. 4. Architecture overview of the TemporalMaxer [48]. The authors propose to modify the transformer of the ActionFormer [62] to employ solely max pooling, removing any self-attention mechanisms from the architecture. Each resulting embedded timestamp within the feature pyramid is then decoded using a classification and a regression head. Note that weights of the decoder are shared across pyramid levels.

TriDet. Similar to the TemporalMaxer, the TriDet model (see Figure 5) suggested to make modifications to the architectural design of the ActionFormer by altering both the encoder and regression head decoder [43]. The authors claim that a transformer-based encoder is prone to suffer from rank loss while simultaneously being high in computational complexity. Consequently, Shi et al. [43] propose replacing the projection and transformer network of the ActionFormer with Scalable-Granularity Perception (SGP) layers. These layers, being fully-convolutional, comprise of two branches: an instant-level branch, which increases the discriminability between the activity classes and the NULL-class, and a window-level branch, aiming to capture semantic context from a wider receptive field. Mathematically, the SGP operator replacing the multi-head attention operator is defined as:

$$f_{SGP} = \phi(x)FC(x) + \psi(x)(Conv_w(x) + Conv_{k \cdot w}(x)) + x \quad (14)$$

, where FC are fully-connected, $Conv_w$ are 1D-depth-wise convolutional layers over the window size w and k is a scalable factor controlling the granularity of captured temporal information. In the TriDet model, the L layers of the feature pyramid $Z = \{z_1, z_2, \dots, z_L\}$ are thus defined as first downsampling the input feature embeddings L times and applying a SGP layer to each downsampled embedding. According to the authors, the ActionFormer architecture suffers from imprecise boundary predictions. To address this, the original regression head is replaced by a Trident-head, which aims to overcome the ActionFormer's shortcomings via an estimated relative probability distribution around each activity boundary. The Trident-head consists of three main components: a start head, responsible for locating the start of an activity segment; an end head, responsible for locating the end of an activity segment; and a center-offset head, responsible for locating the center of an activity segment. Using these three heads, the Trident-head predicts the start (d_t^s) and end boundary (d_t^e) for all L pyramid levels for each timestamp t . Note that all heads, including the classification head, are modelled as three 1D-convolutional layers with parameters shared across all feature pyramid levels.

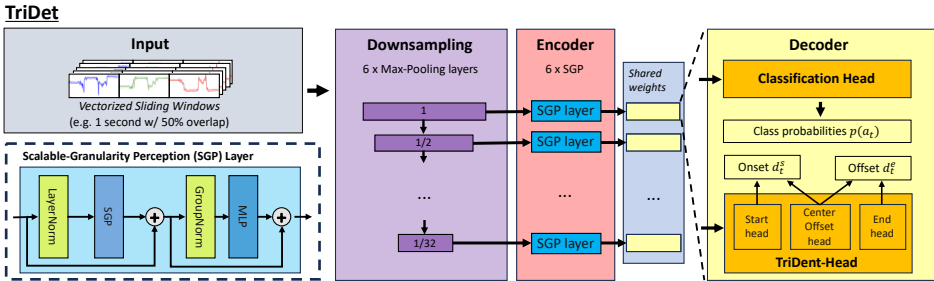


Fig. 5. Architecture overview of the TriDet model proposed by Shi et al. [43]. Compared to the ActionFormer [62], the architecture proposes the following changes: 1. replace the projection and transformer network of the ActionFormer with Scalable-Granularity Perception (SGP) layers along with preceding downsample operators via max-pooling, and 2. replace the regression head with a Trident head, consisting of a start, end and center-offset head. Each resulting embedded timestamp within the feature pyramid is then decoded using the newly defined decoder. Note that weights of the decoder are shared across pyramid levels.

3.4 Similarities and Differences between Inertial and TAL Models

Similar to inertial models, the ActionFormer, TemporalMaxer and TriDet model aim to learn temporal dependencies by learning discriminative feature embeddings. Nevertheless, do the authors credit much of their models' performance to the constructed multi-layer feature pyramid. As

described above, the feature pyramid within each of the three models downsamples the input embedding multiple times in order to create embedding vectors of different temporal granularity. Though this is similar to downsampling performed by concatenating multiple convolution layers without padding, as demonstrated by all inertial architectures in this benchmark analysis, the TAL models use each embedding vector separately instead of only using the resulting embedding vector of the last pyramid layer. More specifically, the authors claim that predicting timestamps at different degrees of temporal granularity holds significant value and is essential in order to correctly predict different types and lengths of activities. Furthermore, as already detailed in previous chapters, the TAL community aims to localize segments rather than provide window-wise predictions. Due to their objective thus differing from that of the inertial community, TAL models are trained not only on a classification loss, but also a regression loss, which optimizes each timestamps corresponding activity onset and offset. Lastly, the use of self-attention based layers has shown to improve results in both communities, yet variations of the ActionFormer show that these layers are not necessarily needed. More specifically, the use of fully-convolutional SGP layers in the TriDet model show that, rather than the type of technique being important, focus needs to be put specifically learning both local and global temporal information for each timestamp.

4 METHODOLOGY

4.1 Datasets

We evaluate each algorithm featured in this benchmark analysis using 6 popular HAR datasets, namely the Opportunity [41], SBHAR [39], Wetlab [42], WEAR [5], Hang-Time [20] and RWHAR dataset [46]. The datasets, all covering different application and recording scenarios, provide us with a challenging set of prediction problems to properly assess the strengths and weaknesses of each model. Table 1 summarizes the key characteristics of each dataset. In addition to vital information such as participant count, activity count, and sensor axes count, the table also includes details on the type of activities found in each dataset. We classify activities into four types: (1) periodic activities, characterized by recurring periodic patterns; (2) non-periodic activities consisting of non-occurring, non-periodical patterns; and (3) complex activities, defined by an arbitrary sequence of non-periodic and periodic activities. Lastly, following the works of Alwassel et al. [2], we provide average count of segments across all subjects, categorizing each segment within each dataset into five bins: XS: (0 seconds, 3 seconds], S: (3 seconds, 6 seconds], M: (6 seconds, 12 seconds], L: (12 seconds, 18 seconds], and XL: more than 18 seconds.

Table 1. Key characteristics of the datasets used in this benchmark analysis. The table provides: participant count (#Sbjs), activity count (#Cls), sensor axes count (#Axes), average number of segments per participant based on absolute length of the segment (#Segments) and type of activities found in the dataset.

Dataset	#Sbjs	#Cls	#Axes	#Segments [2]					Type of Activities
				XS	S	M	L	XL	
Opportunity [41]	4	17(+1)	113	403 ± 63	185 ± 48	48 ± 10	3 ± 2	0 ± 0	non-periodic, complex
SBHAR [39]	30	12(+1)	3	3 ± 2	9 ± 2	6 ± 4	10 ± 4	13 ± 3	periodic, non-periodic
Wetlab [42]	22	8(+1)	3	7 ± 5	7 ± 3	7 ± 2	5 ± 2	13 ± 2	complex
WEAR [5]	18	18(+1)	12	1 ± 1	1 ± 1	1 ± 1	1 ± 1	30 ± 9	periodic
Hang-Time [20]	24	5(+1)	3	154 ± 53	22 ± 7	10 ± 7	3 ± 3	3 ± 2	non-periodic, periodic, complex
RWHAR [46]	15	8	21	0 ± 0	0 ± 0	0 ± 0	0 ± 0	9 ± 1	periodic

Opportunity. Introduced by Roggen et al. [41] in 2010, the Opportunity dataset features a sensor-rich recording scenario of four participants performing various activities of daily living. As part of

this benchmark analysis we chose to use only the sensor subset associated with the Opportunity challenge Chavarriaga et al. [9], which consists of 113 sensor axes from IMU and accelerometer body-worn sensors, all sampling at 30Hz. The Opportunity challenge provides two prediction scenarios, i.e. types of annotations, that is modes of locomotion and gestures. For the benchmark analysis presented in this paper, we focus on the latter, which involves predicting 17 types of activities. The Opportunity dataset was recorded under laboratory-like conditions having each participant take part in six different recording sessions. There were two types of sessions: *ADL sessions*, repeated 5 times, in which participants followed a higher-level protocol and were allowed to interleave activities, and *Drill sessions*, repeated once, in which participants performed a sequence of activities 20 times. Breaks were included in all recording sessions, resulting in a substantial NULL-class being part of the dataset.

SBHAR. Comprising of 30 participants performing six activities of daily living, the SBHAR dataset augments the base locomotion activities with annotated transitional activities, representing transition periods between two base activities [39]. The dataset itself consists of uninterrupted 3D-accelerometer data sampled at 50 Hz, which was captured by a smartphone attached to the waist of each participant. Similar as the Opportunity dataset, the SBHAR dataset was also recorded under laboratory-like conditions, with participants following an experimental protocol that defined repetition count, order and execution length of each activity.

Wetlab. Published by Scholl et al. [42], the Wetlab dataset provides 3D-accelerometer data from 22 participants. A single inertial sensor, placed in a fixed orientation on the dominant wrist of each participant, captured data at a constant sampling rate of 50Hz. The recording of the dataset took place in a wetlab environment in which each participant performed two DNA extraction experiments. Participants were allowed to take as much time as needed for each experiment. However, following an experimental wetlab protocol, recordings of different participants contain almost identical sequences of consecutive activities. Nevertheless, since not all steps in the experimental protocol were mandatory, some activities were skipped by certain participants. The provided annotated activity streams are two-fold, with one set indicating the steps within the recording protocol and the other representing the recurring base activities, such as *peeling*, *pestling*, and *cutting*. During our benchmark analysis the latter will be used, being the 8 base activities (+ the NULL-class), as it is most comparable to the prediction scenarios present in the other benchmark datasets used.

WEAR. Published by Bock et al. [5] in 2023, WEAR consists of 3D-accelerometer and egocentric video data from 18 participants performing 18 workout sports activities at 10 outdoor locations. These activities include running-, stretching- and strength-based exercises, with base activities like push-ups being complemented with complex variations that alter and/ or extend the performed movement during the exercise. The 18 activities were divided across multiple recording sessions, with each session consisting of uninterrupted data streams of all modalities, i.e. including a NULL-class. Although participants were assigned a fixed set of workout activities and instructed to perform each activity for approximately 90 seconds, each participant had the freedom to choose the order of activities and take breaks as desired. During each workout session, four inertial sensors all sampling at 50Hz were placed on both left and right wrists and ankles.

Hang-Time. Published by Hoelzemann et al. [20], Hang-Time features uninterrupted data streams of 24 participants during a basketball practice. The 3D-accelerometer data of each participant was sampled using a smartwatch worn on each participant's right wrist. Although the dataset provides both locomotion and basketball-related activity labels across three different types of sessions (drills, warm-up and game), we intentionally exclude the locomotion activities during our benchmark analysis, replacing them with a NULL-class label. In the drill sessions, participants followed a

strict experimental protocol with predefined activity durations and sequences. In contrast, the warm-up and game sessions allowed participants to commence activities at their discretion in a more real-world recording scenario.

RWHAR. Consisting of 15 participants performing a set of 8 different locomotion activities, the *RWHAR* dataset [46] was recorded at in-the-wild locations. Unlike the other datasets featured in this benchmark analysis, the *RWHAR* dataset does not contain a NULL-class, as recordings were trimmed to only contain the activities of relevancy, cutting out the breaks in-between. Except for jumping, each activity was performed the same amount of time, i.e. around 15 minutes. Participants wore a total of 6 body-worn sensors, all set to sample at 50Hz. During this benchmark analysis, we will only be using the 3D-accelerometer and 3D-gyroscope data provided to make modalities comparable to that of the other datasets.

4.2 Training Pipeline

All experiments were initiated employing a Leave-One-Subject-Out cross-validation. This type of validation involves iteratively training on all but one participant’s data and using the hold-out participant’s data during validation until all participants have been evaluated, ensuring that each network architecture is assessed based on its capabilities to generalize across unseen participants. All datasets were windowed using a sliding window of one second with a 50% overlap across windows. For all inertial architectures [1, 4, 35, 67] we employed a similar optimization as proposed with the release of the shallow DeepConvLSTM, namely an Adam optimizer paired with a learning rate of $1e^{-4}$, a weight decay of $1e^{-6}$, and Glorot weight initialization [15]. To allow each model to converge more properly, we increase the number of epochs to 100 and employ a step-wise learning-rate schedule that multiplies the learning rate by a factor of 0.9 after every 10 epochs. For all architectures, we fixed the hidden dimension of the recurrent layers to employ 128 units and scaled kernel sizes of the convolutional filters according to the relative difference in sampling rate among the different input datasets. In line with how the Attend-and-Discriminate architecture was first introduced, we optimized said architecture using center-loss [54] as opposed to a weighted cross-entropy loss, which was used during training of all other inertial architectures. Lastly, as proposed by the authors, we do not shuffle batches during the training of the shallow DeepConvLSTM.

For all three TAL architectures [43, 48, 62] part of this benchmark analysis, we chose to employ hyperparameters reported by the authors that produced best results on the EPIC-KITCHENS dataset [14]. The hyperparameters, though optimized for a different modality than inertial data (egocentric videos), have shown to produce competitive results on the WEAR dataset [5] and are thus considered a good starting point for evaluating the applicability of the three architectures on other HAR datasets. Nevertheless, given the small size of the tested inertial datasets compared to datasets used by the TAL community, we chose to increase the amount of epochs to 100 throughout all TAL-based experiments. As TAL models are designed to predict both a regression (boundary prediction) and classification target (segment label), loss calculation of the ActionFormer, TemporalMaxer and TriDet models are performed as a weighted combination of a regression loss (IoU loss [40]) and classification loss (focal loss [23]). The latter, originates from the object detection community, which, like HAR, often times suffers from the background class dominating the class distribution. Furthermore, as we treat each subject’s data as a continuous data stream, we apply the TAL models to predict each subject’s data as a whole. With the input sequences thus being of arbitrary length, the ActionFormer, TemporalMaxer and TriDet model limit their complexity by randomly truncating the input sequence to not exceed a maximum sequence length during training. Furthermore, center sampling is employed when training the three TAL models. This technique makes it such that only time steps within an interval around a segment’s center are to be considered positive, while all

other parts are considered negative. Within the TAL community, center sampling has shown to encourage higher scores around activity centers and overall improve results [49, 63].

As inertial models are tasked to predict on a per-window basis and, in most cases, are trained using shuffled data, the architectures suffer from producing only small coherent segments. Caused by frequently occurring activity switches, the fragmentation ultimately leads to significantly lower mAP scores being produced by the inertial architectures as opposed to the TAL models. Therefore, to remove only short lasting switches, predictions of inertial-based architectures mentioned in this paper were smoothed using a majority-vote filter. The exact size of the majority filter was chosen dataset-specific, being, for example, 15 seconds in the case of the WEAR dataset. Similar to the inertial models, the TAL architectures are tasked to predict class probabilities and segment boundaries of each windowed timestamp. Consequently, without applying any confidence threshold, all predicted activity segments are considered during creation of the prediction timeline causing accuracy of the NULL-class to be significantly low. Therefore, to alleviate this, we apply an optimized confidence threshold on predicted segments of all TAL models. Similarly to the majority filter, the score threshold for each architecture was chosen dataset-specific, being, for instance, 0.2 in the case of the WEAR dataset. This eliminates low scoring segments and substantially lowers the confusion of the NULL-class with the other activities.

5 RESULTS

As part of our experimental evaluation, we provide traditional classification metrics (precision, recall and F1-score), misalignment measures as defined by Ward et al. [53] and mAP averaged across tIoU thresholds 0.3, 0.4, 0.5, 0.6 and 0.7. All results are the unweighted average across all subjects along the LOSO validation. Experiments were repeated three times employing three different random seeds (1, 2 and 3). Classification metrics are calculated on a per-sample basis as the segmented output of the TAL models and windowed output of the inertial-models need to be translated to a common time granularity. To ensure readability of this work, visualization of the per-class analysis will only include confusion matrices of the SBHAR and RWHAR datasets, as we deemed these two datasets to be the most representative in illustrating the strengths and weaknesses of the TAL architectures when applied to inertial data. Please note that the confusion matrices of the other datasets can be found in the supplementary material. Furthermore, all created plots part of a performed DETAD analysis [2] on each dataset can be found in our repository.

Per-Dataset Results. Table 2 provides average results of the seven tested architectures across each dataset. One can see that the TAL architectures outperform the inertial architectures across all datasets regarding average mAP. This shows that by being trained to specifically optimize activity boundaries, the different prediction target has resulted in overall more coherent segments which overlap to a larger degree with the ground truth segments. Even though prediction results of the inertial architectures were further smoothed by a majority filter, average mAP is, except for the WEAR dataset, more than halved when compared to that of the TAL architectures. Regarding traditional classification metrics the TAL architectures are able to outperform inertial architectures for four out of six datasets with only the RWHAR [46] and WEAR dataset [5] being the exception. These improvements range between 5% for the Opportunity and Wetlab dataset, 10% for the Hang-Time and even as much as 25% in F1-score for the SBHAR dataset. Calculated misalignment ratios show that both inertial and TAL architectures have a similar distribution of errors, with architectures producing better overall classification results also showing overall lower misalignment measures. Only for the RWHAR dataset one can see that TAL architectures show a significantly higher Overfill-Ratio. This might be due to the RWHAR dataset not featuring a NULL-class, which introduces an uncommon prediction scenario for the TAL architectures. Nevertheless, the performed

DETAD analysis [2], which further differentiates amongst the segment-based errors, reveals that inertial architectures suffer more severely from background errors, i.e. confusing activities with the NULL-class. While this effect is decreased for the shallow DeepConvLSTM, TAL architectures show to be able to more reliably differentiate between activities and the NULL-class, and thus more reliably localize activities within the untrimmed sequences.

Per-Class Results. Figures 6 and 7 show the confusion matrices of the TAL and inertial architectures obtained on the SBHAR and RWHAR datasets. With the improvements on the SBHAR being the largest across all datasets, one can see that this increase can be attributed to improved performance on transitional, non-periodic classes like *sit-to-stand*. These activities are mostly recognisable by their context and surrounding activities and are thus particularly challenging to predict for models that do not rely on temporal dependencies spanning multiple seconds. Since the DeepConvLSTM, Attend-and-Discriminate and TinyHAR models are being trained on shuffled training data and have recurrent parts applied on within-window sequences, the three architectures cannot learn to predict these activities based on surrounding context. Among inertial models, only the shallow DeepConvLSTM is able to more reliably predict these context-based classes as it is trained on unshuffled data and applies a dimensional flip when training the LSTM. Across all datasets part of this benchmark analysis, the RWHAR dataset yields the least performant results for the TAL architectures. We accredit this primarily due to the absence of a NULL-class in the dataset, which introduces a uncommon prediction scenario for the models. Furthermore, the RWHAR consists of the least amount of segments per subject, limiting the amount of training segments which can be used to optimize the TAL models. Results on the RWHAR dataset are nevertheless surprising as the TAL models show confusion among classes which they do not struggle to predict in other datasets (e.g., *lying* in the SBHAR dataset) as well as classes that are not similar to each other (e.g., *lying* and *jumping*). The obtained results raise the question of whether TAL models are primarily suited for being applied on untrimmed sequences, which (1) include breaks and/ or (2) provide a larger amount of segments than the RWHAR dataset.

Nevertheless, apart from the RWHAR dataset, the TAL models deliver the most consistent results across all classes. Even though, in most cases, the individual per-class accuracies are not the highest when compared to results obtained using the inertial architectures, the inertial architectures are frequently not able to predict all classes reliably, with at least one class showing low prediction accuracy. This is especially evident when examining the results obtained on the Hang-Time and Opportunity datasets, where TAL models are capable of correctly predicting challenging non-periodic activities such as *rebounds*, *passes*, *opening door* and *closing door*. Furthermore, as also seen in the DETAD analysis, TAL models are overall more capable of differentiating activities from the NULL-class, showing the highest NULL-class accuracy across all datasets. To summarize, the TAL architectures are more reliable in recognizing any kind of actions within an untrimmed sequence, and are less prone to predict fragmented prediction streams or non-existent breaks.

6 DISCUSSION & CONCLUSION

This article demonstrated the applicability of vision-based, single-stage Temporal Action Localization for inertial-based Human Activity Recognition. We showed that three state-of-the-art TAL models [43, 48, 62] can be applied in a plain fashion to raw inertial data and achieve competitive results on six popular inertial HAR datasets [5, 20, 39, 41, 42, 46], outperforming in most cases popular models from the inertial community by a significant margin. A previously unexplored metric in inertial-based HAR, mean Average Precision (mAP), reveals that TAL models predict less fragmented timelines compared to inertial models and overall achieve larger degrees of overlap with ground truth segments. Furthermore, TAL models show to predict even non-periodic and complex

Table 2. Average LOSO results obtained on six inertial HAR benchmark datasets [5, 20, 39, 41, 42, 46] for four inertial [1, 4, 35, 67] and three TAL architectures [43, 48, 62]. The table provides per-sample classification metrics, i.e. Precision (P), Recall (R), F1-Score (F1), misalignment ratios [53] and average mAP applied at different tIoU thresholds (0.3:0.1:0.7). All experiments employed a sliding window of one second with a 50% overlap. Results are averaged across three runs employing different random seeds. The TAL architectures are able to outperform the inertial architectures regarding average mAP on all HAR datasets and result in the highest classification metrics on four out of the six datasets. Best results per dataset are in **bold**.

	Model	P (↑)	R (↑)	F1 (↑)	UR (↓)	OR (↓)	DR (↓)	IR (↓)	FR (↓)	MR (↓)	mAP (↑)
Opportunity	DeepConvLSTM	50.22	33.88	34.41	0.30	17.29	0.78	31.26	0.01	0.23	13.97
	Shallow D.	42.08	27.18	26.46	0.24	14.28	0.97	35.06	0.01	0.15	10.61
	A-and-D	35.25	48.55	36.35	0.32	15.28	0.45	52.55	0.02	0.35	13.75
	TinyHAR	48.09	54.27	47.09	0.34	19.99	0.39	34.01	0.02	0.46	19.78
	ActionFormer	54.63	58.78	51.93	0.19	13.34	0.41	33.82	0.01	0.42	51.24
	TemporalMaxer	44.44	55.63	44.74	0.21	14.13	0.40	43.78	0.01	0.55	46.31
	TriDet	48.72	57.69	48.79	0.23	13.20	0.39	40.07	0.01	0.58	49.70
SBHAR	DeepConvLSTM	67.54	63.72	62.31	0.41	7.19	0.59	21.44	0.07	0.10	49.60
	Shallow D.	72.98	75.41	71.13	0.60	10.19	0.46	14.23	0.02	0.09	65.15
	A-and-D	68.64	71.07	66.49	0.31	9.47	0.45	21.71	0.05	0.11	55.79
	TinyHAR	58.91	63.70	56.29	0.31	8.16	0.54	31.67	0.05	0.13	45.38
	ActionFormer	87.02	84.37	84.43	0.36	5.41	0.16	5.09	0.00	0.20	95.46
	TemporalMaxer	86.52	83.37	83.66	0.41	6.02	0.19	4.41	0.00	0.24	94.39
	TriDet	88.95	86.15	86.45	0.38	5.41	0.12	3.95	0.01	0.29	94.75
Wetlab	DeepConvLSTM	38.65	47.34	37.87	0.51	7.13	0.69	48.53	0.21	0.64	11.88
	Shallow D.	39.01	35.42	34.42	0.51	9.52	1.57	34.51	0.06	0.43	15.40
	A-and-D	37.75	55.71	37.49	0.56	9.69	0.63	57.60	0.16	0.57	12.27
	TinyHAR	34.31	50.84	31.48	0.61	8.41	1.00	61.26	0.11	0.59	10.05
	ActionFormer	40.71	49.25	40.71	0.56	9.41	0.79	52.44	0.07	0.79	33.53
	TemporalMaxer	50.43	36.65	37.09	0.59	9.37	0.83	53.59	0.10	0.61	35.72
	TriDet	44.13	49.15	42.85	0.58	8.85	0.75	48.63	0.10	0.84	34.05
WEAR	DeepConvLSTM	80.68	76.25	75.78	0.28	2.35	0.52	6.68	0.11	0.32	61.03
	Shallow D.	80.78	78.91	77.71	0.27	3.23	0.50	5.21	0.04	0.43	67.89
	A-and-D	82.34	83.29	80.61	0.20	4.03	0.33	7.18	0.09	0.52	64.78
	TinyHAR	81.87	84.23	80.56	0.21	4.77	0.27	9.54	0.10	0.55	63.33
	ActionFormer	71.88	76.70	72.43	0.22	6.48	0.65	7.12	0.01	2.06	73.80
	TemporalMaxer	69.54	72.80	69.52	0.23	6.87	0.83	5.50	0.01	1.50	69.18
	TriDet	73.57	77.54	73.18	0.28	4.79	0.64	6.21	0.03	1.64	77.12
Hang-Time	DeepConvLSTM	44.13	33.95	35.25	0.28	10.60	0.88	20.16	0.27	1.46	5.44
	Shallow D.	37.97	38.19	36.85	0.35	14.00	1.07	36.38	0.21	2.33	5.00
	A-and-D	40.54	43.32	40.39	0.35	14.14	0.72	34.81	0.30	1.44	6.73
	TinyHAR	37.09	41.13	36.89	0.41	11.59	0.75	42.90	0.43	1.26	4.73
	ActionFormer	49.19	57.57	51.23	0.62	11.63	0.51	47.65	0.48	0.64	29.26
	TemporalMaxer	45.01	54.56	47.17	0.71	10.97	0.45	52.71	1.13	0.65	27.86
	TriDet	49.59	55.14	50.67	0.73	9.85	0.52	48.55	0.69	0.62	29.24
RWHAR	DeepConvLSTM	79.05	81.93	77.56	0.65	2.05	1.09	13.63	1.07	0.00	0.11
	Shallow D.	88.59	89.01	86.85	0.31	1.14	0.38	6.93	0.98	0.00	0.00
	A-and-D	79.46	82.68	78.09	0.66	2.31	1.17	11.28	0.84	0.00	0.04
	TinyHAR	83.59	86.25	82.62	0.53	1.14	0.76	11.65	0.89	0.00	0.02
	ActionFormer	63.76	67.64	61.24	2.48	11.12	2.06	11.23	0.09	0.00	65.40
	TemporalMaxer	63.20	67.60	60.59	2.59	11.95	1.81	13.96	0.36	0.05	50.60
	TriDet	69.27	73.04	67.86	1.48	6.88	2.03	10.24	0.23	0.00	69.98

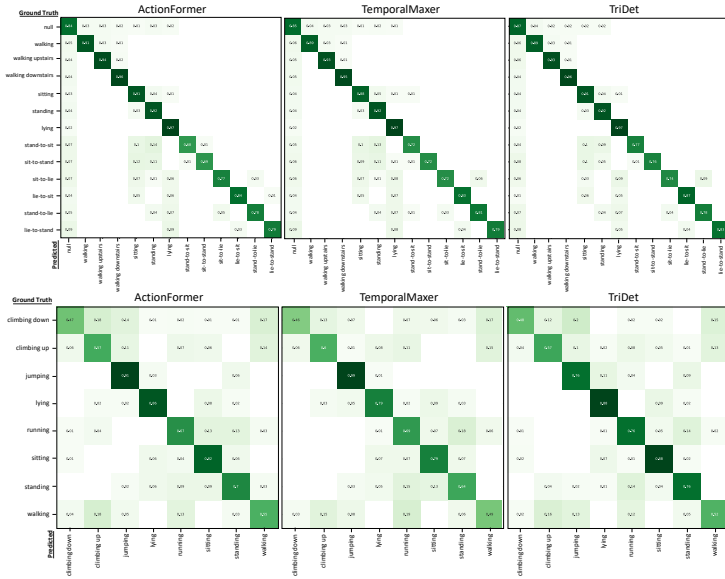


Fig. 6. Confusion matrices of the ActionFormer [62], TemporalMaxer [48] and TriDet model [43] applied on the SBHAR [39] (top) and RWHAR dataset [46] (bottom) with a one second sliding window and 50% overlap. Results are postprocessed using a score threshold of 0.3 in case of the SBHAR dataset. Note that confusions which are 0 are omitted.

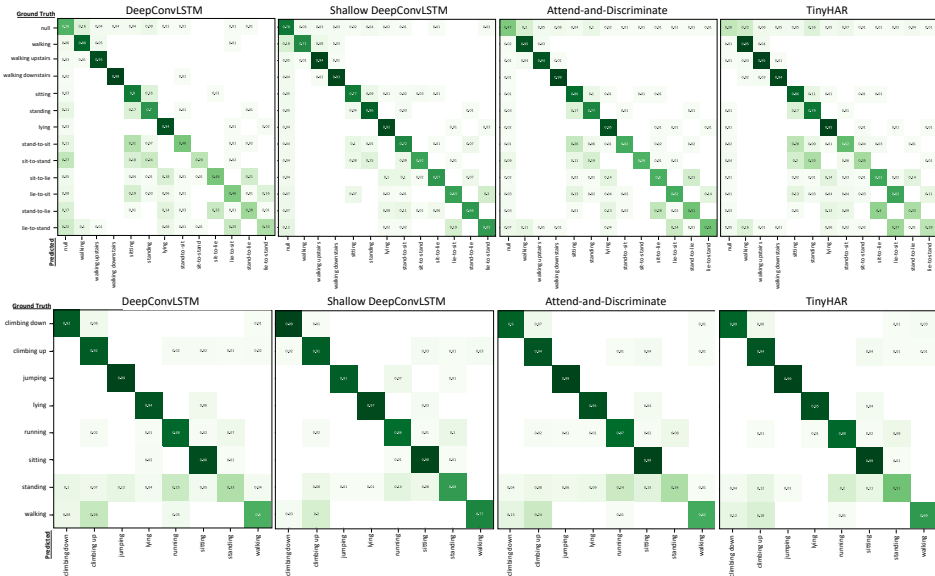


Fig. 7. Confusion matrices of the DeepConvLSTM [35], shallow DeepConvLSTM [4], Attend-and-Discriminate [1] and TinyHAR model [67] applied on the SBHAR [39] (top) and RWHAR dataset [46] (bottom) with a one second sliding window and 50% overlap. Results are postprocessed using a majority filter 5 seconds in case of the SBHAR dataset. Note that confusions which are 0 are omitted.

activities more reliably than inertial architectures, providing consistent results across all types of classes across all datasets. Being one of the key challenges in HAR [7], the TAL architectures further show to be less affected by the unbalanced nature of HAR datasets due to a large NULL-class. Across the five benchmark datasets which offered a NULL-class, the TAL architectures showed to deliver the highest NULL-class accuracy.

Within the past years inertial-based HAR has been working on improving upon methods to model temporal relationships, such as using Transformers as opposed to LSTMs to handle longer sequences [67]. Nevertheless, as also evident from this benchmark analysis, the way these mechanisms are used in popular inertial models does not give them the capability to learn temporal context beyond the current timestamp which is to be predicted [36]. This causes predicted timelines to suffer from frequent activity switches. Even though researchers have suggested new metrics [52], traditional classification metrics remain the focus of analyses within the inertial community. These metrics, though providing a good intuition about the overall recognition performance, do not provide any insight about the degree of fragmentation of the predicted timeline. With researchers such as Pellatt and Roggen [36] and Guan and Plötz [18] having worked on implementing improved training strategies, inertial architectures by default still lack to incorporate context-aware information into their models. Nevertheless, results obtained using the shallow DeepConvLSTM demonstrate that inertial models can be set to learn temporal context, yet require more segment-based optimization to be comparable to TAL architectures as far as average mAP scores.

To summarize, the way TAL architectures are trained does not allow them to be applied in an online fashion. Furthermore, comparing learnable parameters of TAL and inertial models, the former is substantially larger and thus is not suited to be deployed on edge devices. Nevertheless, the retrospective analysis of a fully-captured timeline performed by the TAL community along with fast training times even on large sequences offers an interesting new perspective to inertial-based HAR. Results show that these types of models are leveraging context-based information and are able to outperform popular inertial models on a variety of datasets. Even though models of the two independent communities are sharing similarities, the TAL community offers many unexplored design choices and training concepts, which should be considered to be investigated by the inertial-based HAR community.

REFERENCES

- [1] Alireza Abedin, Mahsa Ehsanpour, Qinfeng Shi, Hamid Reza Tofighi, and Damith C. Ranasinghe. 2021. Attend and discriminate: Beyond the state-of-the-art for human activity recognition using wearable sensors. *ACM on Interactive, Mobile, Wearable and Ubiquitous Technologies* 5, 1 (2021), 1–22. <https://doi.org/10.1145/3448083>
- [2] Humam Alwassel, Fabian Caba Heilbron, Victor Escorcia, and Bernard Ghanem. 2018. Diagnosing error in temporal action detectors. In *European Conference on Computer Vision*. https://doi.org/10.1007/978-3-030-01219-9_16
- [3] Yueran Bai, Yingying Wang, Yunhai Tong, Yang Yang, Qiyue Liu, and Junhui Liu. 2020. Boundary content graph neural network for temporal action proposal generation. In *European Conference on Computer Vision*. https://doi.org/10.1007/978-3-030-58604-1_8
- [4] Marius Bock, Alexander Hoelzemann, Michael Moeller, and Kristof Van Laerhoven. 2021. Improving Deep Learning for HAR with Shallow LSTMs. In *ACM International Symposium on Wearable Computers*. <https://doi.org/10.1145/3460421.3480419>
- [5] Marius Bock, Hilde Kuehne, Kristof Van Laerhoven, and Michael Moeller. 2023. WEAR: An outdoor sports dataset for wearable and egocentric activity recognition. *CoRR* abs/2304.05088 (2023). <https://arxiv.org/abs/2304.05088>
- [6] Navaneeth Bodla, Bharat Singh, Rama Chellappa, and Larry S. Davis. 2017. Soft-NMS – improving object detection with one line of code. In *IEEE International Conference on Computer Vision*. <https://doi.org/10.1109/iccv.2017.593>
- [7] Andreas Bulling, Ulf Blanke, and Bernt Schiele. 2014. A tutorial on human activity recognition using body-worn inertial sensors. *Comput. Surveys* 46, 3 (2014), 1–33. <https://doi.org/10.1145/2499621>
- [8] Joao Carreira and Andrew Zisserman. 2017. Quo vadis, action recognition? A new model and the kinetics dataset. In *IEEE Conference on Computer Vision and Pattern Recognition*. <https://doi.org/10.1109/cvpr.2017.502>

- [9] Ricardo Chavarriaga, Hesam Sagha, Alberto Calatroni, Sundara Tejaswi Digumarti, Gerhard Tröster, José del R. Millán, and Daniel Roggen. 2013. The Opportunity challenge: A benchmark database for on-body sensor-based activity recognition. *Pattern Recognition Letters* 34, 15 (2013). <https://doi.org/10.1016/j.patrec.2012.12.014>
- [10] Guo Chen, Yin-Dong Zheng, Limin Wang, and Tong Lu. 2022. DCAN: Improving Temporal Action Detection via Dual Context Aggregation. In *AAAI Conference on Artificial Intelligence*. <https://doi.org/10.1609/aaai.v36i1.19900>
- [11] Ling Chen, Rong Hu, Menghan Wu, and Xin Zhou. 2023. HMGAN: A hierarchical multi-modal generative adversarial network model for wearable human activity recognition. *ACM on Interactive, Mobile, Wearable and Ubiquitous Technologies* 7, 3 (2023). <https://doi.org/10.1145/3610909>
- [12] Ling Chen, Yi Zhang, Shenghuan Miao, Sirou Zhu, Rong Hu, Liangying Peng, and Mingqi Lv. 2023. SALIENCE: An unsupervised user adaptation model for multiple wearable sensors based human activity recognition. *IEEE Transactions on Mobile Computing* 22, 9 (2023). <https://doi.org/10.1109/TMC.2022.3171312>
- [13] Ling Chen, Yi Zhang, and Liangying Peng. 2020. METIER: A deep multi-task learning based activity and user recognition model using wearable sensors. *ACM on Interactive, Mobile, Wearable and Ubiquitous Technologies* 4, 1 (2020). <https://doi.org/10.1145/3381012>
- [14] Dima Damen, Hazel Doughty, Giovanni Maria Farinella, Antonino Furnari, Jian Ma, Evangelos Kazakos, Davide Moltisanti, Jonathan Munro, Toby Perrett, Will Price, and Michael Wray. 2022. Rescaling egocentric vision: Collection, pipeline and challenges for EPIC-KITCHENS-100. *International Journal of Computer Vision* 130 (2022). <https://doi.org/10.1007/s11263-021-01531-2>
- [15] Xavier Glorot and Yoshua Bengio. 2010. Understanding the Difficulty of Training Deep Feedforward Neural Networks. In *International Conference on Artificial Intelligence and Statistics*. <http://proceedings.mlr.press/v9/glorot10a>
- [16] Guoqiang Gong, Liangfeng Zheng, and Yadong Mu. 2020. Scale matters: Temporal scale aggregation network for precise action localization in untrimmed videos. In *IEEE International Conference on Multimedia and Expo*. <https://doi.org/10.1109/ICME46284.2020.9102850>
- [17] Kristen Grauman, Andrew Westbury, Eugene Byrne, Zachary Chavis, Antonino Furnari, Rohit Girdhar, Jackson Hamburger, Hao Jiang, Miao Liu, and Xingyu Liu. 2022. Ego4D: Around the world in 3,000 hours of egocentric video. In *IEEE/CVF Conference on Computer Vision and Pattern Recognition*. <https://doi.org/10.1109/CVPR52688.2022.01842>
- [18] Yu Guan and Thomas Plötz. 2017. Ensembles of Deep LSTM Learners for Activity Recognition using Wearables. *ACM on Interactive, Mobile, Wearable and Ubiquitous Technologies* 1, 2 (2017), 1–28. <https://doi.org/10.1145/3090076>
- [19] Fabian Caba Heilbron, Juan Carlos Niebles, Victor Escorcia, and Bernard Ghanem. 2015. ActivityNet: A large-scale video benchmark for human activity understanding. In *IEEE Conference on Computer Vision and Pattern Recognition*. <https://doi.org/10.1109/cvpr.2015.7298698>
- [20] Alexander Hoelzemann, Julia L. Romero, Marius Bock, Kristof Van Laerhoven, and Qin Lv. 2023. Hang-time HAR: A benchmark dataset for basketball activity recognition using wrist-worn inertial sensors. *Sensors* 23, 13 (2023). <https://doi.org/10.3390/s23135879>
- [21] Y.-G. Jiang, J. Liu, A. Roshan Zamir, G. Toderici, I. Laptev, M. Shah, and R. Sukthankar. 2014. THUMOS challenge: Action recognition with a large number of classes. <http://csrcv.ucf.edu/THUMOS14/>
- [22] Andrej Karpathy, Justin Johnson, and Fei-Fei Li. 2015. Visualizing and Understanding Recurrent Networks. *CoRR* abs/1506.02078 (2015). <http://arxiv.org/abs/1506.02078>
- [23] Xiang Li, Wenhai Wang, Lijun Wu, Shuo Chen, Xiaolin Hu, Jun Li, Jinhui Tang, and Jian Yang. 2020. Generalized focal loss: Learning qualified and distributed bounding boxes for dense object detection. In *Advances in Neural Information Processing Systems*. https://proceedings.neurips.cc/paper_files/paper/2020/file/f0bda020d2470f2e74990a07a607ebd9-Paper.pdf
- [24] Chuming Lin, Jian Li, Yabiao Wang, Ying Tai, Donghao Luo, Zhipeng Cui, Chengjie Wang, Jilin Li, Feiyue Huang, and Rongrong Ji. 2020. Fast learning of temporal action proposal via dense boundary generator. In *IEEE Conference on Computer Vision and Pattern Recognition*. <https://doi.org/10.1609/aaai.v34i07.6815>
- [25] Chuming Lin, Chengming Xu, Donghao Luo, Yabiao Wang, Ying Tai, Chengjie Wang, Jilin Li, Feiyue Huang, and Yanwei Fu. 2021. Learning salient boundary feature for anchor-free temporal action localization. In *IEEE/CVF Conference on Computer Vision and Pattern Recognition*. <https://doi.org/10.1109/cvpr46437.2021.00333>
- [26] Tianwei Lin, Xiao Liu, Xin Li, Errui Ding, and Shilei Wen. 2019. BMN: Boundary-matching network for temporal action proposal generation. In *IEEE/CVF International Conference on Computer Vision*. <https://doi.org/10.1109/iccv.2019.00399>
- [27] Qinying Liu and Zilei Wang. 2020. Progressive boundary refinement network for temporal action detection. In *AAAI Conference on Artificial Intelligence*. <https://doi.org/10.1609/aaai.v34i07.6829>
- [28] Shengzhong Liu, Shuochao Yao, Jinyang Li, Dongxin Liu, Tianshi Wang, Huajie Shao, and Tarek Abdelzaher. 2020. GlobalFusion: A global attentional deep learning framework for multisensor information fusion. *ACM on Interactive, Mobile, Wearable and Ubiquitous Technologies* 4, 1 (2020). <https://doi.org/10.1145/3380999>

- [29] Xiaolong Liu, Yao Hu, Song Bai, Fei Ding, Xiang Bai, and Philip H. S. Torr. 2021. Multi-shot temporal event localization: A benchmark. In *IEEE/CVF Conference on Computer Vision and Pattern Recognition*. <https://doi.org/10.1109/cvpr46437.2021.01241>
- [30] Xiaolong Liu, Qimeng Wang, Yao Hu, Xu Tang, Shiwei Zhang, Song Bai, and Xiang Bai. 2022. End-to-end temporal action detection with transformer. *IEEE Transactions on Image Processing* 31 (2022). <https://doi.org/10.1109/TIP.2022.3195321>
- [31] Fuchen Long, Ting Yao, Zhaofan Qiu, Xinmei Tian, Jiebo Luo, and Tao Mei. 2019. Gaussian temporal awareness networks for action localization. In *IEEE/CVF Conference on Computer Vision and Pattern Recognition*. <https://doi.org/10.1109/cvpr.2019.00043>
- [32] Shenghuan Miao, Ling Chen, Rong Hu, and Yingsong Luo. 2022. Towards a dynamic inter-sensor correlations learning framework for multi-sensor-based wearable human activity recognition. *ACM Interactive, Mobile, Wearable and Ubiquitous Technologies* 6, 3 (2022). <https://doi.org/10.1145/3550331>
- [33] Vishvak S. Murahari and Thomas Plötz. 2018. On attention models for human activity recognition. In *ACM International Symposium on Wearable Computers*. <https://doi.org/10.1145/3267242.3267287>
- [34] Sauradip Nag, Xi Tian Zhu, Yi-Zhe Song, and Tao Xiang. 2022. Proposal-free temporal action detection via global segmentation mask learning. In *European Conference on Computer Vision*. https://doi.org/10.1007/978-3-031-20062-5_37
- [35] Francisco Javier Ordóñez and Daniel Roggen. 2016. Deep Convolutional and LSTM Recurrent Neural Networks for Multimodal Wearable Activity Recognition. *Sensors* 16, 1 (2016). <https://doi.org/10.3390/s16010115>
- [36] Lloyd Pellatt and Daniel Roggen. 2020. CausalBatch: Solving Complexity/Performance tradeoffs for deep convolutional and LSTM networks for wearable activity recognition. In *ACM International Joint Conference on Pervasive and Ubiquitous Computing and ACM International Symposium on Wearable Computers*. <https://doi.org/10.1145/3410530.3414365>
- [37] Liangying Peng, Ling Chen, Zhenan Ye, and Yi Zhang. 2018. AROMA: A deep multi-task learning based simple and complex human activity recognition method using wearable sensors. *ACM on Interactive, Mobile, Wearable and Ubiquitous Technologies* 2, 2 (2018). <https://doi.org/10.1145/3214277>
- [38] Zhiwu Qing, Haisheng Su, Weihao Gan, Dongliang Wang, Wei Wu, Xiang Wang, Yu Qiao, Junjie Yan, Changxin Gao, and Nong Sang. 2021. Temporal context aggregation network for temporal action proposal refinement. In *IEEE/CVF Conference on Computer Vision and Pattern Recognition*. <https://doi.org/10.1109/cvpr46437.2021.00055>
- [39] Jorge-L. Reyes-Ortiz, Luca Oneto, Albert Samà, Xavier Parra, and Davide Anguita. 2016. Transition-Aware Human Activity Recognition Using Smartphones. *Neurocomputing* 171 (2016). <https://doi.org/10.1016/j.neucom.2015.07.085>
- [40] Hamid Reza Tofighi, Nathan Tsoi, JunYoung Gwak, Amir Sadeghian, Ian Reid, and Silvio Savarese. 2019. Generalized intersection over union: A metric and a loss for bounding box regression. In *IEEE/CVF Conference on Computer Vision and Pattern Recognition*. <https://doi.org/10.1109/cvpr.2019.00075>
- [41] Daniel Roggen, Alberto Calatroni, Mirco Rossi, Thomas Holleczeck, Kilian Förster, Gerhard Tröster, Paul Lukowicz, David Bannach, Gerald Pirkel, Alois Ferscha, Jakob Doppler, Clemens Holzmann, Marc Kurz, Gerald Holl, Ricardo Chavarriaga, Hesam Sagha, Hamidreza Bayati, Marco Creatura, and José del R. Millán. 2010. Collecting Complex Activity Datasets in Highly Rich Networked Sensor Environments. In *IEEE Seventh International Conference on Networked Sensing Systems*. <https://doi.org/10.1109/INSS.2010.5573462>
- [42] Philipp M. Scholl, Matthias Wille, and Kristof Van Laerhoven. 2015. Wearables in the Wet Lab: A Laboratory System for Capturing and Guiding Experiments. In *ACM International Joint Conference on Pervasive and Ubiquitous Computing*. <https://doi.org/10.1145/2750858.2807547>
- [43] Dingfeng Shi, Yujie Zhong, Qiong Cao, Lin Ma, Jia Li, and Dacheng Tao. 2023. TriDet: Temporal action detection with relative boundary modeling. In *IEEE/CVF Conference on Computer Vision and Pattern Recognition*. <https://doi.org/10.1109/cvpr52729.2023.01808>
- [44] Dingfeng Shi, Yujie Zhong, Qiong Cao, Jing Zhang, Lin Ma, Jia Li, and Dacheng Tao. 2022. ReAct: Temporal action detection with relational queries. In *European Conference on Computer Vision*. https://doi.org/10.1007/978-3-031-20080-9_7
- [45] Deepak Sridhar, Niamul Quader, Srikanth Muralidharan, Yaoxin Li, Peng Dai, and Juwei Lu. 2021. Class semantics-based attention for action detection. In *IEEE/ CVF International Conference on Computer Vision*. <https://doi.org/10.1109/iccv48922.2021.01348>
- [46] Timo Szttyler and Heiner Stuckenschmidt. 2016. On-body localization of wearable devices: An investigation of position-aware activity recognition. In *IEEE International Conference on Pervasive Computing and Communications*. <https://doi.org/10.1109/PERCOM.2016.7456521>
- [47] Jing Tan, Jiaqi Tang, Limin Wang, and Gangshan Wu. 2021. Relaxed transformer decoders for direct action proposal generation. In *IEEE/CVF International Conference on Computer Vision*. <https://doi.org/10.1109/iccv48922.2021.01327>
- [48] Tuan N. Tang, Kwonyoung Kim, and Kwanghoon Sohn. 2023. TemporalMaxer: Maximize temporal context with only max pooling for temporal action localization. *CoRR* abs/2303.09055 (2023). <https://arxiv.org/abs/2303.09055>

- [49] Zhi Tian, Xiangxiang Chu, Xiaoming Wang, Xiaolin Wei, and Chunhua Shen. 2022. Fully convolutional one-stage 3D object detection on LiDAR range images. In *Advances in Neural Information Processing Systems*. https://proceedings.neurips.cc/paper_files/paper/2022/file/e1f418450107c4a0ddc16d008d131573-Paper-Conference.pdf
- [50] Yonatan Vaizman, Nadir Weibel, and Gert Lanckriet. 2018. Context recognition in-the-wild: Unified model for multi-modal sensors and multi-label classification. *ACM on Interactive, Mobile, Wearable and Ubiquitous Technologies* 1, 4 (2018). <https://doi.org/10.1145/3161192>
- [51] Ashish Vaswani, Noam Shazeer, Niki Parmar, Jakob Uszkoreit, Llion Jones, Aidan N Gomez, Łukasz Kaiser, and Illia Polosukhin. 2017. Attention is all you need. In *Advances in Neural Information Processing Systems*. <https://proceedings.neurips.cc/paper/2017/file/3f5ee243547dee91fbd053c1c4a845aa-Paper.pdf>
- [52] Jamie A. Ward, Paul Lukowicz, and Hans W. Gellersen. 2011. Performance metrics for activity recognition. *ACM Transactions on Intelligent Systems and Technology* 2, 1 (2011). <https://doi.org/10.1145/1889681.1889687>
- [53] Jamie A. Ward, Paul Lukowicz, and Gerhard Tröster. 2006. Evaluating Performance in Continuous Context Recognition Using Event-Driven Error Characterisation. In *Location- and Context-Awareness*. https://doi.org/10.1007/11752967_16
- [54] Yandong Wen, Kaipeng Zhang, Zhifeng Li, and Yu Qiao. 2016. A Discriminative Feature Learning Approach for Deep Face Recognition. In *European Conference on Computer Vision*. 499–515. https://doi.org/10.1007/978-3-319-46478-7_31
- [55] Christoph Wieland and Victor Pankratius. 2023. TinyGraphHAR: Enhancing human activity recognition with graph neural networks. In *IEEE World AI IoT Congress*. <https://doi.org/10.1109/AIIoT58121.2023.10174597>
- [56] Rui Xi, Mengshu Hou, Mingsheng Fu, Hong Qu, and Daibo Liu. 2018. Deep Dilated Convolution on Multimodality Time Series for Human Activity Recognition. In *IEEE International Joint Conference on Neural Networks*. <https://doi.org/10.1109/IJCNN.2018.8489540>
- [57] Kun Xia, Janguang Huang, and Hanyu Wang. 2020. LSTM-CNN architecture for human activity recognition. *IEEE Access* 8 (2020). <https://doi.org/10.1109/ACCESS.2020.2982225>
- [58] Cheng Xu, Duo Chai, Jie He, Xiaotong Zhang, and Shihong Duan. 2019. InnoHAR: A deep neural network for complex human activity recognition. *IEEE Access* 7 (2019). <https://doi.org/10.1109/ACCESS.2018.2890675>
- [59] Mengmeng Xu, Chen Zhao, David S. Rojas, Ali Thabet, and Bernard Ghanem. 2020. G-TAD: Sub-graph localization for temporal action detection. In *IEEE/CVF Conference on Computer Vision and Pattern Recognition*. <https://doi.org/10.1109/cvpr42600.2020.01017>
- [60] Min Yang, Guo Chen, Yin-Dong Zheng, Tong Lu, and Limin Wang. 2023. BasicTAD: an astounding rgb-only baseline for temporal action detection. *Computer Vision and Image Understanding* 232 (2023). <https://doi.org/10.1016/j.cviu.2023.103692>
- [61] Runhao Zeng, Wenbing Huang, Mingkui Tan, Yu Rong, Peilin Zhao, Junzhou Huang, and Chuang Gan. 2019. Graph convolutional networks for temporal action localization. In *IEEE/CVF International Conference on Computer Vision*. <https://doi.org/10.1109/iccv.2019.00719>
- [62] Chen-Lin Zhang, Jianxin Wu, and Yin Li. 2022. ActionFormer: Localizing moments of actions with transformers. In *Lecture Notes in Computer Science*. https://doi.org/10.1007/978-3-031-19772-7_29
- [63] Shifeng Zhang, Cheng Chi, Yongqiang Yao, Zhen Lei, and Stan Z. Li. 2020. Bridging the gap between anchor-based and anchor-free detection via adaptive training sample selection. In *IEEE/CVF Conference on Computer Vision and Pattern Recognition*. <https://doi.org/10.1109/cvpr42600.2020.00978>
- [64] Ye Zhang, Longguang Wang, Huiling Chen, Aosheng Tian, Shilin Zhou, and Yulan Guo. 2022. IF-ConvTransformer: A framework for human activity recognition using IMU fusion and ConvTransformer. *ACM on Interactive, Mobile, Wearable and Ubiquitous Technologies* 6, 2 (2022). <https://doi.org/10.1145/3534584>
- [65] Chen Zhao, Ali K. Thabet, and Bernard Ghanem. 2021. Video self-stitching graph network for temporal action localization. In *IEEE/CVF International Conference on Computer Vision*. <https://doi.org/10.1109/iccv48922.2021.01340>
- [66] Peisen Zhao, Lingxi Xie, Chen Ju, Ya Zhang, Yanfeng Wang, and Qi Tian. 2020. Bottom-up temporal action localization with mutual regularization. In *European Conference on Computer Vision*. https://doi.org/10.1007/978-3-030-58598-3_32
- [67] Yexu Zhou, Haibin Zhao, Yiran Huang, Till Riedel, Michael Hefenbrock, and Michael Beigl. 2022. TinyHAR: A lightweight deep learning model designed for human activity recognition. In *ACM International Symposium on Wearable Computers*. <https://doi.org/10.1145/3544794.3558467>
- [68] Zixin Zhu, Wei Tang, Le Wang, Nanning Zheng, and Gang Hua. 2021. Enriching local and global contexts for temporal action localization. In *IEEE/CVF International Conference on Computer Vision*. <https://doi.org/10.1109/iccv48922.2021.01326>